Glycoconjugates (Yamakawa, T., Osawa, T., & Handa, S., Eds.) pp 333–334, Scientific Societies Press, Tokyo.
Sharom, F. J., & Grant, C. W. M. (1977) *Biochem. Biophys. Res. Commun. 74*, 1039–1045.
Svennerholm, L. (1957) *Biochim. Biophys. Acta 24*, 604–611.
Von Nicolai, H., Müller, H. E., & Zilliken, F. (1978) *Hoppe-Seyler's Z. Physiol. Chem. 359*, 393–398.
Wiegandt, H., & Baschang, G. (1965) *Z. Naturforsch. B: Anorg. Chem., Org. Chem., Biochem., Biophys., Biol. 20*, 164–166.

Electron Paramagnetic Resonance and Optical Spectroscopic Evidence for Interaction between Siroheme and Tetranuclear Iron–Sulfur Center Prosthetic Groups in Spinach Ferredoxin–Nitrite Reductase†

James O. Wilkerson, Peter A. Janick, and Lewis M. Siegel*

ABSTRACT: Spinach ferredoxin–nitrite reductase (NiR) is a monomeric enzyme containing one siroheme (high-spin Fe^{3+}) and one oxidized Fe_4S_4 cluster per active molecule. When NiR is photochemically reduced with ethylenediaminetetraacetate (EDTA)–deazaflavin, the free enzyme and its CN^- complex display two phases of reduction by visible absorption spectroscopy. The second phase in both cases shows changes in absorption bands associated with the heme even though the heme is already in the Fe^{2+} state. Similarly, the CO complex of NiR, which is formed only when the heme is in the Fe^{2+} state, shows changes in heme absorption bands upon reduction. In the CO and CN^- complexes, these spectral changes are associated with the appearance of electron paramagnetic resonance (EPR) signals of the classical "$g = 1.94$" type characteristic of reduced Fe_4S_4 clusters. The line shapes and exact g values of these EPR signals vary between the two complexes. The second phase of reduction of free NiR is associated with the appearance of three distinct EPR signals: a small $g = 1.94$ type signal (0.11 spin per heme); a signal of the novel type previously observed in the *Escherichia coli* and spinach sulfite reductases (SiRs, also siroheme–Fe_4S_4 enzymes) with $g_\perp = 2.40$ and $g_\parallel = 2.19$ (0.15 spin per heme); an "$S = 3/2$" type signal with $g = 5.07$, 2.91, and 2.09 (0.44 spin per heme), which is similar to the two $S = 3/2$ signals found in *E. coli* SiR. Fully reduced NiR in the presence of 20% dimethyl sulfoxide has greater spin concentration in its $g = 2.40$ ($S = 1/2$) type signal ($g_\perp = 2.35$, $g_\parallel = 2.12$; 0.32 spin per heme) than free NiR. In the presence of 5 mM KCl, the $S = 3/2$ and $S = 1/2$ signals are enhanced while the $g = 1.94$ type signal is diminished. After either treatment, the enzyme remains active. These data suggest the presence of a strong magnetic interaction between the siroheme and Fe_4S_4 centers in spinach NiR. It is suggested that the novel EPR signals of reduced free NiR arise from exchange interaction between $S = 1$ or 2 ferroheme and $S = 1/2$ reduced Fe_4S_4.

Spinach NiR[1] (EC 1.7.7.1) is a monomeric enzyme of 61 000 daltons [Vega & Kamin, 1977; but see Hirasawa-Soga & Tamura (1982) for evidence that the native molecular weight of NiR is 84 000] that catalyzes the six-electron reduction of NO_2^- to NH_3 and SO_3^{2-} to S^{2-} with either reduced ferredoxin or MV^+ as electron donor. It contains a catalytic unit consisting of one siroheme and one Fe_4S_4 cluster per polypeptide (Lancaster et al., 1979; Hirasawa & Tamura, 1980; Knaff et al., 1980). The *Escherichia coli* SiR hemoprotein[2] (Siegel et al., 1982) and spinach SiR (Krueger & Siegel, 1982a) also contain this set of prosthetic groups.

To study this catalytic center further, it is desirable to be able to reduce these enzymes at both iron centers. Unfortunately, the classical strong reductant dithionite is an unsuitable agent, since one of its oxidation products is SO_3^{2-}, a substrate for each of these enzymes (with a K_m much higher than that for NO_2^- in the case of NiR), thus effecting a turnover state that contains little reduced Fe_4S_4 (Siegel et al., 1973, 1982; Vega & Kamin, 1977). MV^+ in equilibrium with H_2 and hydrogenase produced a small $g = 1.94$ type signal, typical of reduced Fe_4S_4 clusters, in these enzymes (Siegel et al., 1982; Lancaster et al., 1979), but quantitative production of such a signal had only been achieved for enzyme complexed with CO (Lancaster et al., 1979; Siegel et al., 1982) until Janick & Siegel (1982) applied the photochemical reducing system described by Massey & Hemmerich (1978) to *E. coli* SiR hemoprotein. This system, of very negative reduction potential, utilizes photoactivated Dfl to extract an electron from EDTA, whereupon it is converted to the strongly reducing Dfl radical species. These radicals react with each other to form a stable dimer species when removed from the light.

Mössbauer studies on *E. coli* SiR hemoprotein have shown that the siroheme and Fe_4S_4 centers are exchange coupled, probably through a bridging ligand, both in oxidized and two-electron-reduced uncomplexed enzyme (Christner et al., 1981). Janick & Siegel (1982, 1983) have reported three novel EPR signals associated with fully reduced SiR: one with $g = 2.53$, 2.29, and 2.07 ($S = 1/2$ type signal) and two with presumed $S = 3/2$ ground state with features at $g = 5.23$ and

† From the Department of Biochemistry, Duke University Medical Center, and the Veterans Administration Hospital, Durham, North Carolina 27705. *Received March 31, 1983.* This work was supported by Grant PCM-7924877 from the National Science Foundation and Project Grant 7875-01 from the Veterans Administration.

[1] Abbreviations: Dfl, 5′-deazaflavin; Fe_4S_4, tetranuclear iron–sulfur center; Fe_2S_2, binuclear iron–sulfur center; MV^+, reduced methyl viologen; NiR, nitrite reductase; SiR, sulfite reductase; EDTA, ethylenediaminetetraacetic acid; Me_2SO, dimethyl sulfoxide; EPR, electron paramagnetic resonance.

[2] The hemoprotein is a subunit of the native enzyme that is multimeric as isolated, having an $\alpha_8\,\beta_4$ subunit structure (Siegel et al., 1973, 1982; Siegel & Davis, 1974). The flavoprotein (α_8) moiety accepts electrons from NADPH, the physiological donor. The isolated monomeric hemoprotein (β) subunit is fully catalytically competent in the presence of a suitable electron donor, such as MV^+ (Siegel et al., 1982).

0006-2960/83/0422-5048$01.50/0

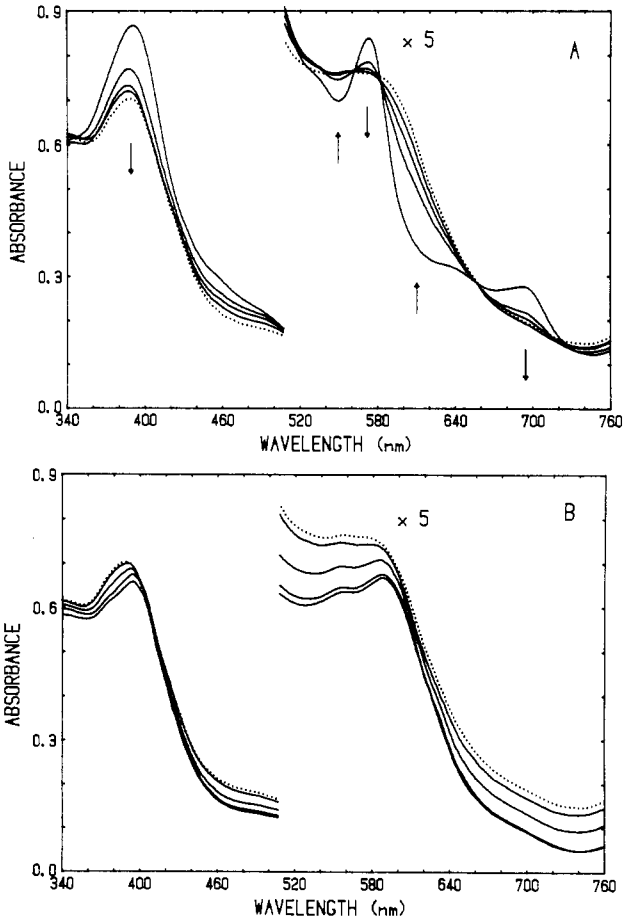

FIGURE 1: Optical spectra of NiR during photoreduction with Dfl–EDTA. A solution containing 39 μM NiR, 20 μM Dfl, and 1 mM EDTA in standard buffer was made anaerobic in a quartz EPR tube (effective path length approximately 3 mm) and illuminated for 15–30-s intervals. After each interval, the visible absorption spectrum was recorded. The dotted spectrum (···) represents the 75-s illumination time point in both (A) and (B) (see text). The bottom spectrum of (B) was recorded after 3.5-min illumination. No change in this spectrum was observed upon an additional 3-min illumination. (A) Spectra of the first phase of reduction. Arrows point from the fully oxidized spectrum toward spectra of increasing illumination time. (B) Spectra of the second phase of reduction. Successive spectra show reduced absorbance.

2.80 and at $g = 4.82$ and 3.39. The $S = 1/2$ signal was considered by Christner et al. (1981) to represent that of the coupled reduced Fe_4S_4 ($S = 1/2$)–ferroheme ($S = 1$ or 2) system.[3] Fully reduced spinach SiR also displays a novel $S = 1/2$ EPR signal with $g = 2.48$, 2.34, and 2.08.

In the present work, we have investigated the optical and EPR properties of spinach NiR in the native enzyme and its complexes with CN^- and CO. Reduced native NiR displays novel EPR signals of both the $S = 1/2$ and $S = 3/2$ type, which are similar to but distinct from those of the SiRs. Analysis of spectral changes indicates that interaction between the heme and Fe_4S_4 centers exists in NiR as in the *E. coli* and spinach SiRs.

Experimental Procedures

Spinach NiR was purified by the method of Lancaster et al. (1981). Enzyme concentration was determined using $\epsilon_{386} = 7.6 \times 10^4\ M^{-1}\ cm^{-1}$ (Lancaster et al., 1979). The standard

[3] The $S = 3/2$ signals were as yet undiscovered at the time the work of Christner et al. (1981) was published. However, the existence of these signals is compatible with this coupling model [see Janick & Siegel (1982, 1983)].

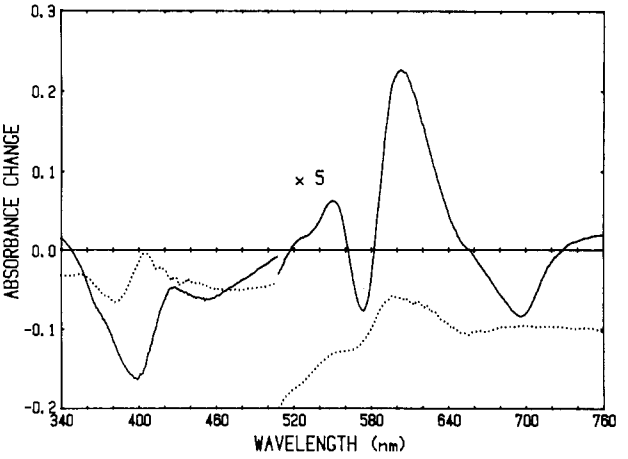

FIGURE 2: Optical difference spectra between successive NiR oxidation states. Spectra were calculated from the spectra of Figure 1 with the aid of a computer as described under Experimental Procedures. The first (oxidized) spectrum of Figure 1A was subtracted from the 60-s illumination spectrum (most reduced solid-line spectrum in Figure 1A) to produce the 1-e–0-e spectrum (—). The most oxidized solid-line spectrum of Figure 1B (1.5-min illumination) was subtracted from the most reduced spectrum (3.5-min illumination) to produce the 2-e–1-e spectrum (···).

buffer used in all experiments was 0.1 M potassium phosphate–0.1 mM EDTA, pH 7.7. Dfl was the generous gift of Dr. David Seybert. All other chemicals were reagent grade and used without further purification.

Anaerobic photoreduction of NiR solutions in EPR tubes or optical cuvettes was achieved by the method of Massey & Hemmerich (1978). Anaerobic techniques and the recording of optical spectra in EPR tubes were as previously described by Janick & Siegel (1982).

Optical spectra were recorded at room temperature on an Aminco DW-2 dual-beam spectrophotometer. EPR spectra were recorded at X-band with a Varian E-9 spectrometer equipped with an Air Products liquid helium cryostat. Modulation frequency was 100 kHz, and modulation amplitude was 10 G in all experiments. Spin concentrations were determined from spectra recorded under nonsaturating conditions either by double integration or by integration of isolated absorption-type peaks according to the method of Aasa & Vänngård (1975). A solution of cupric EDTA was used as a spin-concentration standard. The following temperatures and microwave powers were used for quantitation of the various EPR signals reported here: high-spin ferriheme, $g = 2.40$ type signals and $g = 1.94$ type signals, 20 K and 50 mW; $S = 3/2$ type signals, 8 K and 100 mW. A Hewlett-Packard 9825A computer equipped with a 9874A digitizer and 7225A graphics plotter was used for translation of spectra into digital format to facilitate calculation of optical difference spectra and integration of EPR spectra. A modified version of the program of Lowe (1978) was used for EPR spectral simulations.

Results

Photoreduction of NiR. Spinach NiR is readily reduced by illumination of the enzyme in the presence of Dfl and EDTA with the procedure of Massey & Hemmerich (1978). This process can be followed with optical spectroscopy and, after the sample is frozen, by EPR spectroscopy. The visible absorption spectra of native NiR at successive stages of photoreduction are shown in Figure 1. Difference spectra computed between the successive spectra indicate a dramatic change in the nature of the reductive process after the spectrum designated by the dotted line in Figure 1. This suggests that

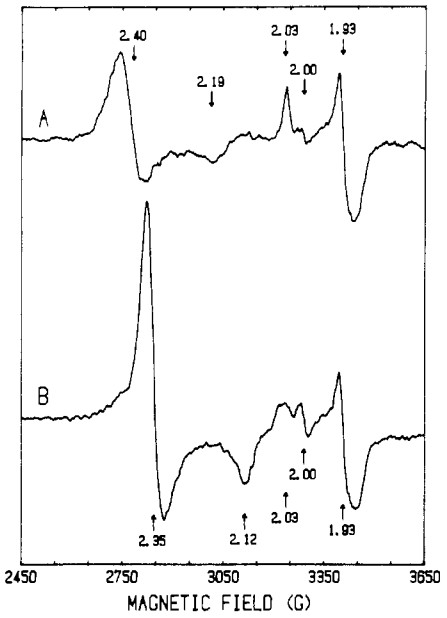

FIGURE 3: EPR spectra (20 K) of fully reduced spinach NiR in standard buffer an in standard buffer plus 20% Me_2SO. (Top) After the spectra of Figure 1 were recorded, the EPR tube containing the fully photoreduced sample was frozen in liquid N_2 and the EPR spectrum recorded. (Bottom) A quartz EPR tube containing 34.8 μM NiR, 10 μM Dfl, and 0.9 mM EDTA in standard buffer plus 20% Me_2SO was made anaerobic and illuminated in 0.5–1-min intervals, and its optical spectrum was monitored until no further optical change was observed (spectra obtained following 12- vs. 15-min illumination were identical) and the EPR spectrum recorded. The conditions of measurement for both spectra were as follows: temperature 20 K; microwave power 50 mW. The feature at $g = 2.00$ represents a small amount of radical that can be seen in photoreduced samples from which enzyme has been omitted.

reduction occurs in at least two phases corresponding to the difference spectra seen in Figure 2. In the first phase of the reduction process (Figures 1A and 2), declines at the Soret (386 nm) and α-band (573 nm) maxima are associated with only slight shifts in the positions of these maxima.[4] The absorption band at 691 nm is also lost during this phase. A similar feature has been observed in the optical spectra of the siroheme-containing SiRs from spinach (Krueger & Siegel, 1982b) and *E. coli* (Janick & Siegel, 1982), as well as Fe–isobacteriochlorin model complexes (Stolzenberg et al., 1981), only when the heme iron is in the high-spin ferric state. This phase of enzyme reduction is also associated with increased absorbance in the 520–560-nm and 580–650-nm regions. EPR spectra of NiR recorded during this first phase are associated with loss of the high-spin ferriheme signal at $g = 6.78$, 5.17, and 1.98, characteristic of the oxidized enzyme, with no new signals arising.

The second phase of photoreduction (Figures 1B and 2) is characterized by further diminutions of absorbance and marked shifts in the positions of the Soret (to 394 nm) and α-band (to 588 nm) maxima. An absorbance maximum at 557 nm also gains prominence. There are no apparent isosbestic points associated with this phase.[5] The difference spectrum associated with the second phase of reduction (Figure 2, dotted line) is more complex, particularly above 500 nm, than the relatively featureless decrease in absorbance ("bleaching") associated with the reduction of most Fe_4S_4 clusters previously studied. This suggests that changes in the spectrum of the siroheme occur in this phase of reduction, as well as in the first.

Three distinct EPR signals arise essentially in parallel during the second phase of reduction. The upper spectrum of Figure 3 was taken under conditions that emphasize two of these signals. One is nearly axial with $g_\parallel = 2.03$ and $g_\perp = 1.93$, characteristic of the reduced Fe_4S_4 clusters in a number of reduced iron–sulfur proteins. However, the integrated spin intensity of this signal compared to the others (Table I) shows that the species giving rise to it represents only a small pro-

Table I: Integrated EPR Spin Intensities as a Fraction of Total Siroheme in Maximally Reduced Nitrite Reductase Samples

	additions to enzyme[a]		
EPR species	none	20% Me_2SO	5 mM KCl
$S = 3/2$	0.44	0.23	0.71
$S = 1/2$	0.15[b]	0.32[c]	0.22[b]
$g = 1.94$	0.11	0.10	0.08
total	0.70	0.65	1.01

[a] For details of procedures used for generating photoreduced samples and for recording EPR spectra of individual signal types, refer to the text and to the legends of Figures 3 and 4. Integrated EPR spin intensities were determined as described under Experimental Procedures. [b] $g_\perp = 2.40$ and $g_\parallel = 2.19$. [c] $g_\perp = 2.35$ and $g_\parallel = 2.12$.

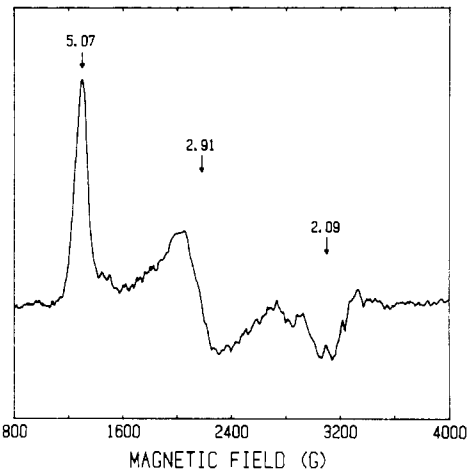

FIGURE 4: EPR spectrum of fully reduced NiR at 8 K. A quartz EPR tube containing 77.8 μM NiR, 40 μM Dfl, and 1 mM EDTA in standard buffer was made anaerobic and illuminated for 90 min, after which an optical spectrum was recorded. No change in this spectrum was observed following a further 30-min illumination. The optical spectrum of the sample was identical with the most reduced spectrum of Figure 1. The sample was then frozen in liquid N_2 and the EPR spectrum recorded. Conditions of measurement were as follows: temperature 8 K; microwave power 100 mW.

[4] Apparent isosbestic points are present during the first reductive phase at 562, 582, and 728 nm. However, these spectra (Figure 1A) are not isosbestic in the region near 500 nm. Preliminary data from this laboratory show that freshly isolated "free" NiR displays in the earliest stages of reduction an EPR signal assigned by Aparicio et al. (1975) to the ferroheme–NO complex of the enzyme (J. O. Wilkerson and L. M. Siegel, unpublished results). Thus, the apparent lack of isosbesticity near 500 nm may be related to a fraction of the enzyme bound with substrate [NO_2^- (?)], which is reduced and dissociates from the enzyme during the experiment.

[5] On reoxidation of the enzyme with potassium ferricyanide, the intensity of the original oxidized NiR is not fully restored (although the shape and positions of the absorbance maxima are restored). Recovery, judged by comparing the initial and final absorbances at the Soret maximum at 386 nm, is generally in the range of 85–95%. This result suggests that some fraction (~10%) of the enzyme is irreversibly destroyed during photoreduction. Thus, the calculated difference spectrum in Figure 2 corresponding to 2-e – 1-e enzyme (dotted line) may reflect in part a difference spectrum of denatured vs. intact enzyme (reduction state not specified). Enzyme reduced no farther than the end of the first phase (Figure 1A) is fully recoverable on reoxidation.

portion of the total sample. The other signal in Figure 3, top, is also nearly axial, with $g_\perp = 2.40$ and $g_\parallel = 2.19$. This novel type of EPR signal has previously been observed, with slightly differing g values and line shapes, in the assimilatory SiR of spinach (Krueger & Siegel, 1982b) and the hemoprotein subunit of *E. coli* SiR (Janick & Siegel, 1982, 1983). The $g = 1.94$ and $g = 2.40$ signals are highly saturated when the EPR spectrum is recorded at <10 K and high (100-mW) microwave power, and a third type of signal ($g = 5.07$, 2.91, and 2.09) dominates the spectrum (Figure 4). Double integration of this very rhombic signal demonstrates that it in fact represents the majority species in fully reduced uncomplexed NiR (Table I). The positions of the resonances (g_1 and g_2 split about $g = 4$ and $g_3 \approx 2$) suggest this signal represents a species with an $S = 3/2$ ground state.

Janick & Siegel (1982) have observed changes in the relative proportions of the $S = 1/2$ and $S = 3/2$ signals of reduced *E. coli* SiR hemoprotein effected by a variety of agents. The effects on NiR of two of these agents, Me_2SO and KCl, have been studied, and results similar to those seen with SiR have been obtained. No change in the optical spectrum of the enzyme in the presence of either agent was observed at any oxidation state. A NiR sample photoreduced in the presence of 20% Me_2SO yielded the EPR spectrum of Figure 3, bottom. The integrated spin intensities of each signal (Table I, $S = 3/2$ spectrum, not shown in Figure 3) show that the $S = 1/2$ species' signal (g values shifted to $g_\perp = 2.35$, $g_\parallel = 2.12$) is dramatically enhanced at the expense of the $S = 3/2$ species' signal. When 5 mM KCl is present in the photoreduction sample solution, two effects are obvious from the data of Table I: (A) The proportion of total integrated spin intensity associated with the $g = 1.94$ type of signal is decreased from 16% to 8%, while the proportion of spin intensity due to the $S = 3/2$ species is slightly increased (from 63% to 71%), that due to the $S = 1/2$ species remaining essentially unchanged (21–22%) in enzyme photoreduced in the presence or absence of KCl. (B) The reduction of NiR in this sample proceeded apparently quantitatively to completion. This latter effect is quite reproducible and may represent halide stabilization of the enzyme with respect to destruction by the photoreduction process, this destruction giving rise to increased $g = 1.94$ type signal.

NiR–Cyanide Complex. Cyanide added to a sample of oxidized NiR binds rapidly to a single site at the siroheme, inducing a high-spin to low-spin transition of the ferriheme iron (Vega & Kamin, 1977; Aparicio et al., 1975; Cammack et al., 1978; Lancaster et al., 1979). Relative to uncomplexed NiR, the optical spectrum of NiR–CN^- (Figure 5A) displays complete loss of the "charge-transfer" band at 691 nm, as well as decreased absorbance and a substantial shift in the wavelength maximum at the Soret (to 404 nm), increased absorbance at the α-band (576 nm), and the emergence of a distinct β-band at 536 nm. The EPR spectrum of oxidized NiR–CN^- shows resonances typical of low-spin hemes with $g = 2.71$, 2.35, and ~1.8 [spectrum not shown; see Salerno et al. (1979)].

Photoreduction of the complex proceeds in two observable phases, as seen in the optical spectra of Figure 5. The first phase displays isosbestic points at 502 and 547 nm and is associated with the disappearance of the low-spin ferriheme signal. As in the uncomplexed enzyme, the second reductive phase proceeds with no observable isosbestic points. The maximally reduced NiR–CN^- complex displays a split Soret peak (maxima at 404 and 412 nm) and a shoulder at 503 nm in the visible region. The only EPR signal apparently associated with this state of the enzyme is a $g = 1.94$ type signal,

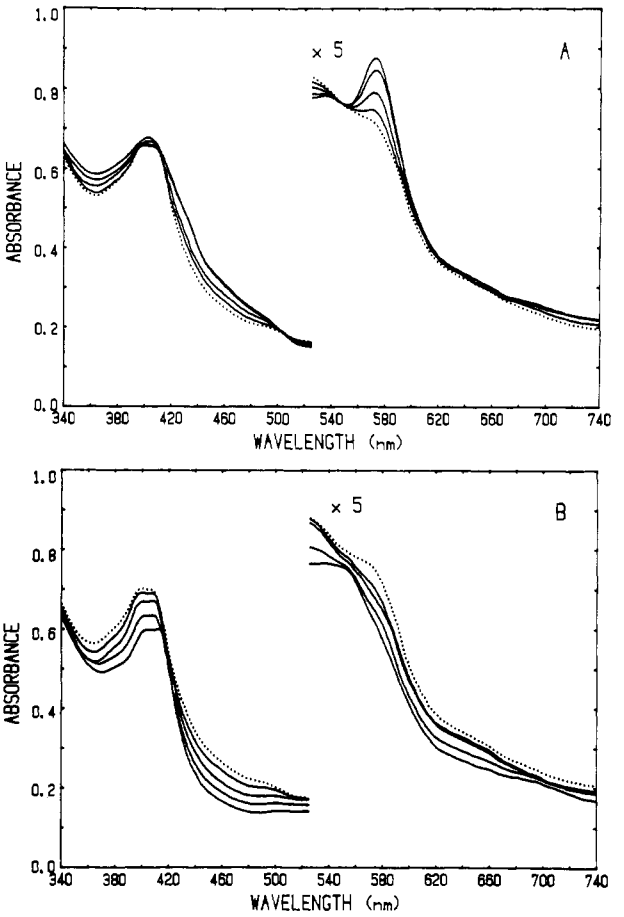

FIGURE 5: Optical spectra of NiR–CN^- complex during photoreduction with Dfl–EDTA. A silica cuvette, 5-mm path length, containing a solution of 22 μM NiR, 10 μM Dfl, 1 mM EDTA, and 100 μM KCN was made anaerobic in the double-cuvette apparatus, which had a syringe needle inserted through both septa to allow addition from a syringe containing anaerobic 78.5 μM $K_3Fe(CN)_6$ in standard buffer. The sample was illuminated for successive 1-min intervals while the optical spectrum was monitored until no further change in the spectrum was observed. The reduced spectrum was recorded, and successive additions of 2 μL of the $K_3Fe(CN)_6$ solution were made, the resulting spectrum recorded after each addition, until no change other than dilution effects were observed in the spectrum. The spectra were corrected for dilution, and difference spectra between each addition were calculated with the aid of a computer. Each difference spectrum up to 6 μL added $K_3Fe(CN)_6$ was qualitatively the same. The difference spectra calculated for 8–20 μL added $K_3Fe(CN)_6$ were likewise similar to each other but quite different from the earlier set. The calculated difference spectrum between 6 and 8 μL added $K_3Fe(CN)_6$ was intermediate between the other two groups. (A) The absorbance spectra of the second oxidative (first reductive) phase. (B) The absorbance spectra of the first oxidative (second reductive) phase. A greater degree of reduction is associated with decreased absorbance at all wavelengths in absorbance spectra of the first oxidative (second reductive) phase. A greater degree of reduction is associated with decreased absorbance at all wavelengths in both (A) and (B) except between 502 and 547 nm in (A). The dotted spectrum (···) is that of the sample after 8 μL added $K_3Fe(CN)_6$ in both graphs.

shown in Figure 6, bottom ($g = 2.0365$, 1.9402, and 1.9191), which was quantitated at 0.31 spin per heme; the $g = 5.07$ and $g = 2.40$ type signals characteristic of free reduced NiR are absent. Oxidative titrations of samples of fully reduced NiR–CN^- in standardized potassium ferricyanide solution indicate that, at most, only 1.4 equiv per heme is required for complete oxidation (data not shown), suggesting that the $g = 1.94$ type EPR signal represents essentially all of the two-electron-reduced enzyme in the sample.

It can be noted from the optical spectra in Figure 5B and the difference spectrum corresponding to the second reductive

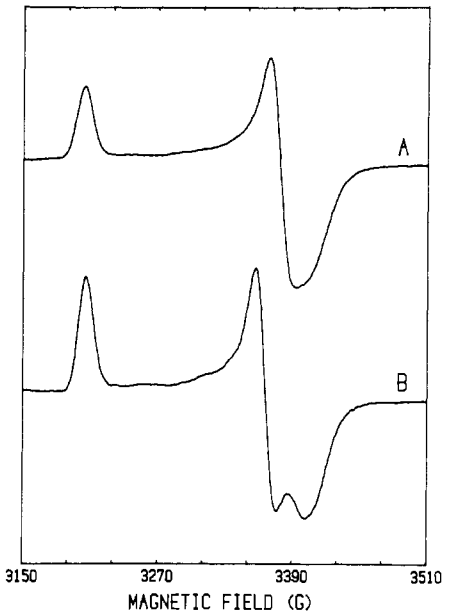

FIGURE 6: EPR spectra of maximally reduced NiR–CO and NiR–CN^- complexes. (A) After the spectra of Figure 8 were recorded, the photoreduced NiR–CO sample in its EPR tube was frozen in liquid N_2 and the EPR spectrum recorded. g values of g = 2.0367, 1.9320, and 1.9179 for this signal were derived by spectral simulation. (B) A quartz EPR tube containing 22 μM NiR, 5 μM Dfl, 10 mM EDTA, and 5 mM KCN was made anaerobic and illuminated until no further change in the optical absorbance spectrum was detected. The shape of the absorbance spectrum at this point was identical with the most reduced spectrum of Figure 5B. The sample was frozen in liquid N_2 and the spectrum recorded. g values from spectral simulation are g = 2.0365, 1.9402, and 1.9191. Conditions of measurement for both spectra were as follows: temperature 20 K; microwave power 50 mW.

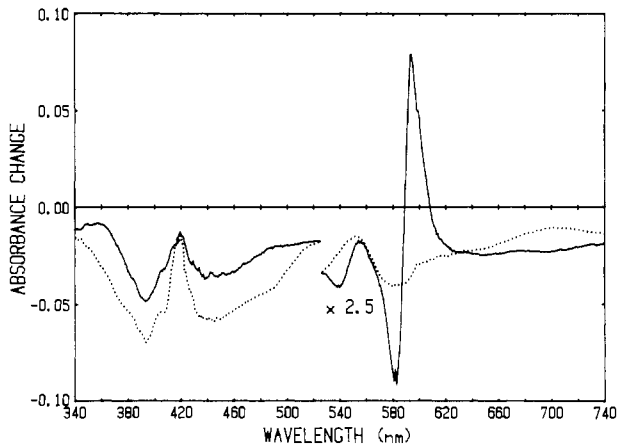

FIGURE 7: Optical difference spectra representing the single phase of NiR–CO complex reduction and the first oxidative phase of maximally reduced NiR–CN^- complex. The NiR–CO spectrum (—) was calculated by using the spectra labeled oxidized and reduced in Figure 8. The NiR–CN^- spectrum (···) was calculated by using the spectrum of fully photoreduced NiR–CN^- complex and the spectrum after 6 μL added $K_3Fe(CN)_6$, the first and fourth solid lines of Figure 5B, respectively. The spectra are normalized to a 3-mm path length.

phase seen in Figure 7 (dotted line) that this phase, associated specifically with Fe_4S_4 cluster reduction by EPR analysis, is also associated with marked qualitative changes in the visible absorption spectrum, especially at wavelengths greater than 500 nm. This suggests that Fe_4S_4 cluster reduction effects changes in the siroheme optical spectrum.

NiR–CO Complex. Vega & Kamin (1977) have shown that CO slowly forms a complex with spinach NiR in which the MV^+/NO_2^- reductase activity of the enzyme disappears. Inhibition by CO required the presence of a reducing agent.

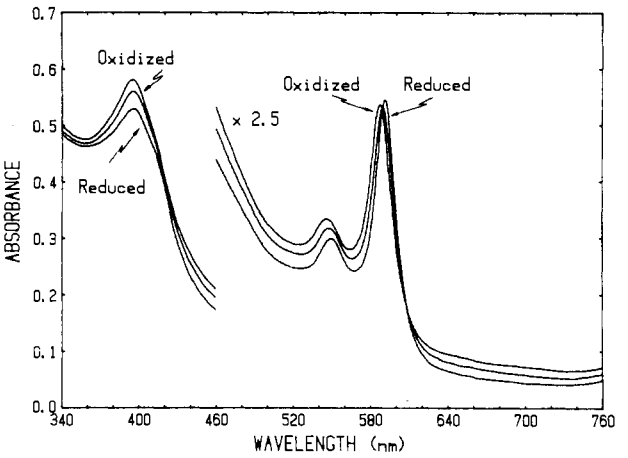

FIGURE 8: Optical spectra of NiR–CO complex during photoreduction with Dfl–EDTA. A quartz EPR tube containing 22 μM NiR, 5 μM Dfl, and 10 mM EDTA was alternately flushed with CO (made oxygen-free by bubbling through a solution of MV^+) and evacuated several times, finally being left under an atmosphere of CO. It was illuminated for 15–30-s intervals and its optical spectrum monitored until the absorbance peak at 691 nm disappeared, when the spectrum labeled oxidized was recorded. The sample was illuminated further and the spectrum recorded after intervals of 30 s. No further changes were observed once the sample displayed the spectrum labeled reduced.

It has also been shown that the NiR–CO complex yields a g = 1.94 type EPR spectrum in the presence of excess reductant that reaches a maximum signal intensity when the strong reducing agent $Na_2S_2O_4$ is added after the complex is formed (Lancaster et al., 1979).

A sample of NiR under a CO atmosphere was photoreduced in steps and its optical spectrum monitored until the charge-transfer band at 691 nm had disappeared. The optical spectrum of the sample at this point in the photoreduction, shown in Figure 8 (labeled oxidized), exhibits absorbance maxima at 587 (α-band), 545 (β-band), and 396 nm (Soret). Further illumination of this sample yielded the remaining spectra of Figure 8. The presence of isosbestic points at 589 and 608 nm indicates the presence of only two species of enzyme contributing to these spectra. On reduction, the absorbance maxima of NiR–CO complex are bathochromatically shifted to 592, 548, and 397 nm for the α-band, β-band, and Soret band, respectively. The introduction of controlled amounts of air to the atmosphere above the sample yielded at the end point a spectrum identical with that labeled oxidized in Figure 8. The spectra of Figure 8 all exhibit a pattern of absorption bands (intense α-band in the 590–610-nm region, smaller β-band in the 540–550-nm region, and Soret at approximately 400 nm) characteristic of siroheme–CO complexes both free in solution (Murphy et al., 1974; Stolzenberg et al., 1981) and in the siroheme-containing sulfite reductases (Siegel, 1978; Krueger & Siegel, 1982b; Janick & Siegel, 1983), indicating that the CO is bound to the heme in both the oxidized and reduced NiR–CO complexes.

The EPR spectrum of oxidized NiR–CO complex is devoid of signals except for a g = 4.3 resonance of small integrated spin intensity, probably due to adventitious ferric iron. This signal is typically found in the EPR spectra of all NiR samples except those frozen in strongly reducing conditions. Fully reduced NiR–CO complex exhibits the g = 1.94 type EPR signal shown in Figure 6, top (g = 2.0367, 1.9320, and 1.9179; integrated spin intensity of 0.56 spin per heme). No signal resembling the g = 2.40 or g = 5.07 signals of uncomplexed NiR nor any other resonance has been detected in the spectrum of this complex.

The EPR evidence presented above indicates that it is re-

duction of the Fe_4S_4 cluster that is responsible for the spectral shifts of Figure 8. The calculated difference spectrum of the reduction of the NiR–CO complex is shown in Figure 7 (solid line). The complexity of this spectrum at wavelengths near the siroheme absorption bands suggests once again that changes in the heme iron's electronic environment are occurring, though its spin and oxidation states remain unchanged. Inspection of the EPR spectra shown in Figure 6 demonstrates that the line shape and g values of the reduced Fe_4S_4 cluster differ with the nature of the ligand at the heme (whether CN^- or CO).

Discussion

Optical and EPR spectra recorded after various illumination times during photoreduction of spinach NiR show that the enzyme is reduced in at least two sequential steps both when uncomplexed and when bound with CN^- ion, a potent inhibitor of catalytic activity. Earlier attempts at photoreduction of uncomplexed NiR failed, apparently due to destruction of the enzyme once it had been reduced by more than one electron per heme. This destruction has been greatly reduced (but not eliminated) by lowering the concentration of EDTA in the photoreduction medium from 10 to 1 mM.

Unlike spinach sulfite reductase and *E. coli* sulfite reductase hemoprotein, both siroheme–Fe_4S_4 proteins, spinach NiR does not require a reducing agent in order to rapidly bind CN^-. Oxidized, aerobic NiR in the presence of excess CN^- rapidly and quantitatively forms a complex in which the heme Fe is converted to low-spin character (Lancaster et al., 1979). This conversion suggests, but does not prove, the CN^- is directly ligated to the heme Fe. Reduction of the NiR–CN^- complex results first in reduction of the ferriheme to a diamagnetic ferroheme species and then in reduction of the Fe_4S_4 cluster to yield a typical $g = 1.94$ type EPR spectrum. Even though the heme Fe is already in the ferrous state during the second phase of reduction, the heme's optical absorption bands undergo marked shifts during this phase, showing that reduction of the Fe_4S_4 cluster is associated with an altering of the electronic environment of the heme.

The binding of CO, another potent inhibitor of catalytic activity, to NiR does require the presence of a reductant, and the resulting complex exhibits a single phase of spectral changes upon photoreduction. The optical spectra of NiR–CO complex (in either oxidized or reduced state) are qualitatively similar to that of free siroheme–CO in aqueous solution (Murphy et al., 1974). Thus it appears that CO, like CN^-, is probably ligated directly to the siroheme Fe of NiR. It is a characteristic of hemoprotein–CO complexes, as contrasted with CN^- complexes, that CO remains tightly bound only to the ferrous state of the heme Fe, so it is not surprising that the NiR–CO complex exhibits only one spectral phase during photoreduction, corresponding to reduction of the Fe_4S_4 cluster. The appearance of a $g = 1.94$ type EPR spectrum upon photoreduction of the NiR–CO complex further shows that the Fe_4S_4 is the reducible center in this case.

The changes seen in the NiR–CN^- and NiR–CO optical spectra accompanying changes in the Fe_4S_4 oxidation state are quite different from the rather general "bleaching" of absorbance in the visible wavelength region usually observed during reduction of iron–sulfur proteins or $Fe_4S_4(SR)_4^{2-}$ model compounds (Palmer, 1975; Holm & Ibers, 1976). Furthermore, the detailed line shapes and g values of the EPR signal of the reduced Fe_4S_4 cluster differ depending on whether CN^- or CO is ligated to the heme Fe. These results suggest that each prosthetic group of NiR is sensitive to the electronic environment and/or oxidation state of the other, i.e., that the two groups interact in some way at the catalytic center of NiR.

A novel $S = 1/2$ type EPR signal with all three g values above 2.0 and a pair of signals of probable $S = 3/2$ ground state have been described for fully reduced uncomplexed *E. coli* SiR by Janick & Siegel (1982, 1983). Mössbauer data of Christner et al. (1981) for that enzyme demonstrate conclusively that during reduction electrons add sequentially to the heme and Fe_4S_4 centers and that the two centers are antiferromagnetically spin coupled in the fully oxidized and fully reduced forms. Coupling in the one-electron-reduced form is strongly implied by their data.[6] Mössbauer spectra of oxidized, uncomplexed NiR using natural abundance ^{57}Fe clearly demonstrate magnetic splitting of the oxidized ($S = 0$) Fe_4S_4 spectrum by the paramagnetic ($S = 5/2$) ferriheme.[7] This splitting is very similar to that found with *E. coli* SiR and is also due to antiferromagnetic spin exchange between the two centers, implying the existence of a chemical link (presumably in the form of a bridging ligand) between them (Cohen, 1980).

The combined EPR and optical spectra obtained during photoreduction of uncomplexed NiR (e.g., loss of the high-spin ferriheme EPR signal and disappearance of the characteristic charge-transfer band at 691 nm) indicate that the heme Fe is reduced prior to the Fe_4S_4 cluster in this enzyme as well. Full reduction of NiR is coincident with the appearance of two signals in the EPR spectrum, which together represent a majority of the two-electron-reduced species, one with $g_\perp = 2.40$ and $g_\parallel = 2.19$ and the other with $g = 5.07$, 2.91, and 2.09, together with a minor proportion of $g = 1.94$ type signal.[8] These signals are qualitatively very similar to the novel $S = 1/2$ and $S = 3/2$ signals found in fully reduced *E. coli* SiR. A novel signal of the $S = 1/2$ type ($g = 2.48$, 2.34, and 2.08) has also been reported for fully reduced spinach SiR (Krueger & Siegel, 1982b). In light of the *E. coli* SiR results, it seems likely that the EPR signals of fully reduced spinach NiR are due to a coupled reduced Fe_4S_4 ($S = 1/2$)–ferroheme ($S = 1$ or 2) system as well. In the reduced NiR–CN^- and –CO complexes, marked changes in the nature of the $g = 1.94$ type EPR spectrum due to exchange coupling (e.g., to a $g = 2.40$ type of signal) would not be expected, since the ferroheme of these complexes is probably in the $S = 0$ state.

The evidence presented in this paper, together with the previously published results for *E. coli* SiR and spinach SiR, suggests that the siroheme–Fe_4S_4 interaction is a general feature of both types of six-electron reductase enzymes.[9]

Acknowledgments

We are grateful to Dr. Michael J. Barber for help with producing the EPR spectral simulations of the reduced NiR–

[6] A discussion of the theoretical relationship between spin-exchange coupling of the Fe_4S_4 and siroheme centers and the EPR signals observed in uncomplexed *E. coli* SiR hemoprotein (Ferriheme signal in the fully oxidized form and novel $S = 1/2$ and $S = 3/2$ ground state signals in fully reduced enzyme) has been presented by Janick & Siegel (1982).

[7] J. A. Christner, E. Münck, J. O. Wilkerson, P. A. Janick, and L. M. Siegel, unpublished results.

[8] The origin of this $g = 1.94$ type signal, also found as a minor component of *E. coli* and spinach SiRs, is unknown. Likely explanations include that is represents enzyme whose Fe_4S_4 and siroheme centers have become uncoupled or, alternatively, that it represents enzyme whose heme is low spin. Small amounts of low-spin ferriheme signal are typically seen in the oxidized EPR spectra of each of these enzymes as isolated.

[9] Cammack et al. (1982) have recently reported that *E. coli* NADH–nitrite reductase contains an Fe_2S_2 cluster of relatively positive midpoint potential, as well as siroheme, FAD, and, apparently, additional nonheme iron [see Jackson et al. (1981)]. The EPR experiments they reported were performed under conditions such that they might well have missed detection of any novel $S = 1/2$ and $S = 3/2$ type signals such as those seen in fully reduced spinach NiR.

CO and NiR–CN^- complexes and to Dr. Christopher J. Batie for supplying some of the purified NiR used in this work.

Registry No. Ferredoxin–nitrite reductase, 37256-44-3; siroheme, 52553-42-1.

References

Aasa, R., & Vänngård, T. (1975) *J. Magn. Reson. 19*, 308–315.

Aparicio, P. S., Knaff, D. B., & Malkin, R. (1975) *Arch. Biochem. Biophys. 169*, 102–107.

Cammack, R., Hucklesby, D. P., & Hewett, E. J. (1978) *Biochem. J. 171*, 519–526.

Cammack, R., Jackson, R. H., Cornish-Bowden, A., & Cole, J. A. (1982) *Biochem. J. 207*, 333–339.

Christner, J. A., Münck, E., Janick, P. A., & Siegel, L. M. (1981) *J. Biol. Chem. 256*, 2098–2101.

Cohen, I. A. (1980) *Struct. Bonding (Berlin) 40*, 1–37.

Hirasawa, A., & Tamura, G. (1980) *Agric. Biol. Chem. 44*, 749–758.

Hirasawa-Soga, A., & Tamura, G. (1982) *Agric. Biol. Chem. 46*, 1319–1328.

Holm, R. H., & Ibers, J. A. (1976) in *Iron–Sulfur Proteins* (Lovenberg, W., Ed.) Vol. 3, pp 205–281, Academic Press, New York.

Jackson, R. H., Cole, J. A., & Cornish-Bowden, A. (1981) *Biochem. J. 193*, 861–867.

Janick, P. A., & Siegel, L. M. (1982) *Biochemistry 21*, 3538–3547.

Janick, P. A., & Siegel, L. M. (1983) *Biochemistry 22*, 504–515.

Knaff, D. B., Smith, J. M., & Chain, R. K. (1980) *Arch. Biochem. Biophys. 199*, 117–122.

Krueger, R. J., & Siegel, L. M. (1982a) *Biochemistry 21*, 2892–2904.

Krueger, R. J., & Siegel, L. M. (1982b) *Biochemistry 21*, 2905–2909.

Lancaster, J. R., Vega, J. M., Kamin, H., Orme-Johnson, M. R., Orme-Johnson, W. H., Krueger, R. J., & Siegel, L. M. (1979) *J. Biol. Chem. 254*, 1268–1272.

Lancaster, J. R., Batie, C. J., Kamin, H., & Knaff, D. B. (1981) in *Methods in Chloroplast Molecular Biology* (Edelmans, M., Halleck, K. B., & Chua, N.-H., Eds.) pp 723–734, Elsevier, Amsterdam.

Lowe, D. J. (1978) *Biochem. J. 171*, 649–651.

Massey, V., & Hemmerich, P. (1978) *Biochemistry 17*, 9–17.

Murphy, M. J., Siegel, L. M., Tove, S. R., & Kamin, H. (1974) *Proc. Natl. Acad. Sci. U.S.A. 71*, 612–616.

Palmer, G. (1975) *Enzymes, 3rd Ed. 12*, 1–56.

Salerno, J. C., Lancaster, J. R., & Kamin, H. (1979) *Abstracts of Papers*, XIth International Conference on Biochemistry, Toronto, p 162.

Siegel, L. M. (1978) in *Mechanisms of Oxidizing Enzymes* (Singer, T. P., & Ondarza, R. N., Eds.) pp 201–214, Elsevier, Amsterdam.

Siegel, L. M., & Davis, P. S. (1974) *J. Biol. Chem. 249*, 1587–1598.

Siegel, L. M., Davis, P. S., & Kamin, H. (1973) *J. Biol. Chem. 248*, 251–264.

Siegel, L. M., Rueger, D. C., Barber, M. J., Krueger, R. J., Orme-Johnson, N. R., & Orme-Johnson, W. H. (1982) *J. Biol. Chem. 257*, 6343–6350.

Stolzenberg, A. M., Strauss, S. H., & Holm, R. H. (1981) *J. Am. Chem. Soc. 103*, 4763–4778.

Vega, J. M., & Kamin, H. (1977) *J. Biol. Chem. 252*, 896–909.